

Linear zeros versus SU(3) in meson-baryon scattering*

H. B. Mathis and R. H. Capps

Physics Department, Purdue University, West Lafayette, Indiana 47907

(Received 26 December 1973)

Odorico has shown that measurements of certain meson-baryon scattering amplitudes support the postulate that the zeros in the spin-independent amplitudes are approximately linear in the Mandelstam plane. He has shown further that if the postulate is extended to all meson-baryon amplitudes, a violation of SU(3) interaction symmetry is implied. We investigate the possibility of determining from experimental data which of the two principles, the linear-zero postulate or SU(3) interaction symmetry, is better satisfied. The reactions $\bar{K}N \rightarrow \pi\Sigma$ and $\pi N \rightarrow K\Sigma$ are crucial in this determination. We show that the existing data involving these processes are not in perfect accord with either of the two principles, but favor the linear-zero postulate.

I. INTRODUCTION

Odorico has cited experimental evidence that the zeros in the spin-independent amplitudes (A) for $\pi N \rightarrow \pi N$, $\bar{K}N \rightarrow \bar{K}N$, and $\bar{K}N \rightarrow \pi\Lambda$ processes are approximately linear in the Mandelstam plane.^{1,2} He identifies these lines of zeros with specific patterns discussed in an earlier paper.³ It is stated in Ref. 1 that with these identifications the hypothesis that all other meson-baryon A amplitudes correspond to allowed linear-zero patterns requires a violation of SU(3) interaction symmetry. However, the data analysis of Odorico of the above-mentioned processes does not in itself require SU(3) violation.

The possibility that nature prefers linear zeros to SU(3) symmetry for these amplitudes is intriguing. The purpose of this paper is to study the question further, and to identify the possible experiments that can best show which, if either, of the principles of linear zeros and SU(3) symmetry is approximately valid. In this connection, existing phase-shift analyses of $\bar{K}N \rightarrow \pi\Sigma$ and $\pi N \rightarrow K\Sigma$ data are compared with the various theoretical predictions.

A brief review of the implications of the linear-zero postulate is given in Sec. II A, and Sec. II B contains a complete list of the assumptions that lead to the conflict with SU(3). The conflict is demonstrated in Sec. III. In Sec. IV B, SU(3)-symmetric solutions for zero patterns and resonance widths in $\bar{K}N \rightarrow \pi\Sigma$ and $\pi N \rightarrow K\Sigma$ amplitudes are derived, and corresponding predictions based on the linear-zero postulate are given in Sec. IV C. These predictions are compared to experiment in Sec. V.

II. PROCEDURE

A. The linear-zero patterns

In order to make clear where the conflict between the linear-zero hypothesis and SU(3) arises, we will express the linear-zero hypothesis in the algebraic form derived in a previous paper.⁴ We modify the notation of Ref. 4 to make it appropriate to meson-baryon scattering. An amplitude in the s , t , and u Mandelstam channels is represented by $a+b-c+d$, $a+\bar{c}-\bar{b}+d$, and $\bar{c}+b-\bar{a}+d$, respectively, where the bar denotes an antiparticle and a and c denote mesons. The spin dependence of an s -channel, meson-baryon scattering amplitude T is represented by

$$T = -A(s, t) + \frac{1}{2}i[\gamma \cdot (q_1 + q_2)]B(s, t),$$

where q_1 and q_2 are the four-momenta of initial and final mesons, and s (t) is the square of the energy in the center-of-mass system for an s - (t -) channel process. As in Ref. 1, we are concerned only with the spin-independent amplitude $A(s, t)$. We use V and T to denote residues of vector and tensor-meson Regge trajectories, respectively, and N and Δ to denote residues of baryon trajectories of the nucleon type (physical particles of $j = \frac{1}{2}, \frac{5}{2}$, etc.) and Δ type ($j = \frac{3}{2}, \frac{7}{2}$, etc.), respectively. In general, each of the N and Δ residues is a sum of contributions from both parities in the direct channel (channel of the physical particles of the trajectory).

The residues are related to coupling constants by the equations

$$\begin{aligned}
T_t &= g_{rd\bar{b}} g_{r\bar{c}a}, & V_t &= g_{rd\bar{b}} g_{r\bar{c}a}, \\
N_s &= g_{rd\bar{c}} g_{rba}, & \Delta_s &= g_{rd\bar{c}} g_{rba}, \\
N_u &= g_{rd\bar{a}} g_{rb\bar{c}}, & \Delta_u &= g_{rd\bar{a}} g_{rb\bar{c}},
\end{aligned} \tag{1}$$

where the index of T , V , N , or Δ is the channel of the physical particles of the trajectory, and a summation over contributing trajectories r is implied.

It is shown in Ref. 4 that the linear-zero hypothesis is equivalent to the requirement that the ratios of residues in the different channels correspond to one of thirteen possibilities, each of which corresponds to a pattern of zeros. These sets of residue ratios, and the directions of the zero lines, are given in Table I.

A normalizing convention has been used to simplify Table I. The linear-zero prescription specifies the ratio of residues of two resonances in different channels at the point of intersection of the resonances. Thus, in pattern I(u), where a V resonance intersects s -channel N and Δ resonances, the requirements for V_t are

$$V_t(\alpha) = N_s(\alpha), \quad V_t(\beta) = \Delta_s(\beta),$$

where α and β are the intersection points in the Mandelstam plane of the vector resonance with the N and Δ resonances, respectively. Actually, $V_t(\alpha)$ and $V_t(\beta)$ are not equal. However, we assume that the ratio of residues of like trajectories is the same at different points, so that the ratio $V_t(\beta)/V_t(\alpha)$ is the same for all V trajectories. Hence, by renormalizing the residues Δ_s , we may write

$$V_t = N_s = \Delta_s \tag{2a}$$

for this pattern, where now V_t denotes $V_t(\alpha)$. We may use Table I only to compare the residues of like trajectories, e.g., we cannot compare a Δ/N ratio with experiment. By a similar argument, the residue N_s is not the same when the N resonance crosses V and T resonances, but we renormalize the T relative to the V so that we may write [for pattern I(u)]

$$N_s = V_t = T_t, \tag{2b}$$

where the residues all refer to the point α . Equations (2a) and (2b) are the ratios of Table I for this pattern.

Since all meson-baryon resonances may be associated with the s channel, we need make little use of the N_u and Δ_u . Two patterns related by the particle permutation $a \rightleftharpoons \bar{c}$ must be related by the permutation $s \rightleftharpoons u$ in the pattern label of Table I.

B. Assumptions

The principal result of Ref. 1 is that SU(3) interaction symmetry for the spin-independent ampli-

tudes is in conflict with the following set of assumptions:

(A) The KN states are exotic.

(B) In each of the πN amplitudes ($\pi^+ p$ scattering, $\pi^0 p$ scattering, and $\pi^- p \rightarrow \pi^0 n$) at least one of the s -channel residues is nonzero.

(C) There are nine V and nine T trajectories, with the isotopic spins and hypercharges of SU(3) octets and singlets.

(D1) The $\pi N \rightarrow \pi N$, $\bar{K} N \rightarrow \bar{K} N$, and $\bar{K} N \rightarrow \pi \Lambda$ amplitudes correspond to linear-zero patterns.

(D2) All other $MB \rightarrow MB$ (where M and B denote a pseudoscalar meson and a member of the nucleon octet) amplitudes also correspond to linear-zero patterns.

III. ORIGIN OF THE CONFLICT

A. The πN and $\bar{K} N$ patterns

There is strong experimental evidence in favor of assumptions (A)–(C) above, and Odorico has demonstrated the approximate validity of assumption (D1).^{1,2} Therefore, we will take these assumptions as given and pinpoint the conflict between assumption (D2) and SU(3) symmetry.

We consider first πN and $\bar{K} N$ scattering. As seen from Table I, assumptions (A) and (D1) imply pattern I(u) for $K^- p$ and $K^- n$ elastic scattering. Odorico points out that assumptions (B) and (D1) imply that $\pi^+ p$ and $\pi^- p$ scattering must correspond to $\text{III}^-(u)$ and $\text{III}^-(s)$, or to $\text{III}^-(s)$ and $\text{III}^-(u)$.¹ Although for our argument concerning the conflict it is irrelevant which of these two assignments is made, it is clearly preferable to assign $\text{III}^-(u)$ to

TABLE I. The residue ratios for the allowed zero patterns. The second column lists the Mandelstam variables that are constant along the different zero lines. Zero lines corresponding to constant differences in Mandelstam variables extend throughout the plane, while those corresponding to constant s , t , or u occur only at negative values of the variable.

Pattern	Zero lines	T_t	V_t	N_s	Δ_s	N_u	Δ_u
I(t)	t	0	0	1	-1	1	-1
I(s)	s	1	-1	0	0	1	1
I(u)	u	1	1	1	1	0	0
$\text{II}^+(t)$	$t, s-u$	2	0	1	1	1	1
$\text{II}^+(s)$	$s, u-t$	1	1	2	0	1	-1
$\text{II}^+(u)$	$u, s-t$	1	-1	1	-1	2	0
$\text{II}^-(t)$	$t, s-u$	0	2	1	1	-1	-1
$\text{II}^-(s)$	$s, u-t$	1	1	0	2	-1	1
$\text{II}^-(u)$	$u, s-t$	1	-1	-1	1	0	2
III^+	s, t, u	1	0	1	0	1	0
$\text{III}^-(t)$	s, t, u	1	0	0	1	0	1
$\text{III}^-(s)$	s, t, u	0	1	1	0	0	-1
$\text{III}^-(u)$	s, t, u	0	-1	0	-1	1	0

$\pi^+ p$ scattering. Otherwise, the $j = \frac{3}{2}$ (Δ) contribution to $\pi^+ p$ scattering would have to be canceled by another Δ -type resonance. Henceforth, we take the $\pi^+ p$ pattern to be $\text{III}^-(u)$.

B. The conflict

In order to demonstrate the conflict, we will assume SU(3) symmetry of the residues and find the implied violation of assumption (D2). For this purpose, we need consider only the t -channel residues V_t and T_t . The pattern assignment $\text{I}(u)$ for $K^- p$ and $K^- n$ scattering implies $V_t = T_t$ for these two processes. This is equivalent to the two conditions

$$\frac{1}{8} d_1 G_1 + \frac{1}{5} d_8 G_8 = \frac{1}{3} f_8 G'_a, \quad (3)$$

$$\frac{1}{8} d_1 G_1 - \frac{1}{10} d_8 G_8 - \left(\frac{1}{20}\right)^{1/2} d_8 G_a = \frac{1}{6} f_8 G'_a - \left(\frac{1}{20}\right)^{1/2} f_8 G'_s, \quad (4)$$

where d_1 , d_8 , and f_8 are the interaction constants of the tensor-singlet, tensor-octet, and vector-octet trajectories with MM states; G_1 , G_8 , and G_a are the coupling constants of the tensor singlet with $B\bar{B}$ states and of the tensor octet with symmetric and antisymmetric $B\bar{B}$ states, while G'_s and G'_a are the corresponding coupling constants of the vector octet with $B\bar{B}$ states. Each constant is normalized so that its square is the sum of the squares of the constants of interactions of one trajectory with all MM or $B\bar{B}$ states. Identification of pattern $\text{III}^-(u)$ with $\pi^+ p$ scattering requires $T_t = 0$; this is the coupling-constant relation

$$\frac{1}{8} d_1 G_1 - \frac{1}{10} d_8 G_8 + \left(\frac{1}{20}\right)^{1/2} d_8 G_a = 0. \quad (5)$$

One may use Eqs. (3), (4), and (5) to solve for the three interaction constants $d_1 G_1$, $d_8 G_8$, and $d_8 G_a$ in terms of $f_8 G'_s$ and $f_8 G'_a$. One finds that the F/D ratios (denoted by x and x') for coupling with baryons are related by

$$x = (1-x')/(1+3x'), \quad (6)$$

where $x = \left(\frac{2}{9}\right)^{1/2} (G_a/G_8)$ and $x' = \left(\frac{5}{9}\right)^{1/2} (G'_a/G'_s)$.

We next consider the process $K^- p \rightarrow \pi^0 \Lambda$, since the A amplitude for this process is analyzed for linear zeros in Ref. 2. The t -channel residues for this amplitude are

$$V_t = \frac{1}{4} \left(\frac{1}{3}\right)^{1/2} f_8 \left[\left(\frac{1}{5}\right)^{1/2} G'_s + G'_a \right], \quad (7)$$

$$T_t = -\frac{1}{4} \left(\frac{2}{5}\right)^{1/2} d_8 \left[\left(\frac{1}{5}\right)^{1/2} G_8 + G_a \right].$$

It can be seen from Table I that in all patterns, the following algebraic condition is satisfied:

$$V_t T_t (V_t + T_t)(V_t - T_t) = 0. \quad (8)$$

Application of this condition to Eqs. (7), together with Eqs. (3)–(5), limits the coupling ratios to

four discrete solutions, characterized by the x' values $\frac{1}{3}$, -1 , $-\frac{1}{3}$, and ∞ . The possibility $x' = -1$ may be discarded, because it corresponds to the decoupling of the ρ trajectory from nucleons, in which case the πN patterns all degenerate into solutions with no nonzero residues, in violation of assumption (B). Thus, the three allowed x' values are

$$x' = \frac{1}{3}, -\frac{1}{3}, \text{ and } \infty. \quad (9)$$

We complete the argument by considering two more A amplitudes. The first corresponds to the process $K^+ \Lambda \rightarrow K^+ \Lambda$, for which the t -channel residues are

$$V_t = \left(\frac{1}{20}\right)^{1/2} f_8 G'_s, \quad T_t = \frac{1}{10} d_8 G_8 + \frac{1}{8} d_1 G_1. \quad (10)$$

The second process is $K^0 \Sigma^+ \rightarrow K^+ \Sigma^0$, for which the t -channel residues are

$$V_t = \left(\frac{1}{18}\right)^{1/2} f_8 G'_a, \quad T_t = -\left(\frac{1}{10}\right)^{1/2} d_8 G_a. \quad (11)$$

It is straightforward to show that for each of the x' values of Eq. (9), the residue ratios determined from Eqs. (3)–(5) are such that the V_t and T_t of at least one of the two processes [of Eqs. (10) and (11)] do not satisfy the condition of Eq. (8). This completes the demonstration of the inconsistency of SU(3) symmetry with the set of assumptions of Sec. II B. Furthermore, we have not applied SU(3) symmetry to the baryonic channels; i.e., the assumptions of Sec. II B are inconsistent with t -channel SU(3).⁵

IV. CONFLICTING PREDICTIONS FOR $N \rightarrow \Sigma$ PROCESSES

A. General considerations

We next discuss the experimental information that can best show whether SU(3) or the linear-zero hypothesis is better satisfied for the A amplitudes. The most suitable amplitudes for this purpose are of the type $\bar{K}N \rightarrow \pi\Sigma$, or the crossed type $\pi N \rightarrow K\Sigma$; we refer to these as $N \rightarrow \Sigma$ amplitudes. The zero patterns and the decay partial widths of resonances of these amplitudes are relevant. In Sec. IV B we show that if SU(3) is combined with Odorico's analysis of the πN and $\bar{K}N$ scattering amplitudes and the $K^- p \rightarrow \pi^0 \Lambda$ amplitude,^{1,2} there are only two solutions for the $N \rightarrow \Sigma$ spin-independent amplitudes. The linear-zero hypothesis is not satisfied for either solution. In Sec. IV C, we outline the argument of Ref. 1 that the linear-zero hypothesis leads to specific predictions for the $N \rightarrow \Sigma$ amplitudes. The predictions of these two subsections are compared with experiment in Sec. V.

B. The SU(3) solutions

Odorico has shown that the πN and $\bar{K}N$ scattering amplitudes are consistent with linear-zero patterns,¹ so we take these amplitudes to correspond to the patterns assigned in Sec. IIIA. In Ref. 2 evidence is given for zeros of constant u and constant ($s-t$) in the A amplitude for $K^-p \rightarrow \pi^0\Lambda$. Consequently, we follow Ref. 1 and assume that this amplitude corresponds to one of the two patterns with such zeros. As seen from Table I these are patterns $\Pi^+(u)$ and $\Pi^-(u)$. Either of these assignments requires $V_t = -T_t$. As seen from Eq. (7), the requirement is

$$\left(\frac{5}{9}\right)^{1/2} f_8 \left[\left(\frac{1}{5}\right)^{1/2} G'_s + G'_a \right] = d_8 \left[\left(\frac{1}{5}\right)^{1/2} G_s + G_a \right]. \quad (12)$$

This equation and Eqs. (3)–(5) lead to the following complete solution for the t -channel residue ratios:

$$d_1 G_1 = 0, \quad d_8 G_8 = \left(\frac{5}{9}\right)^{1/2} f_8 G'_s, \quad (13)$$

$$G'_a/G'_s = G_a/G_s = \left(\frac{1}{5}\right)^{1/2} \quad (\text{or } x' = x = \frac{1}{5}).$$

If duality is applied to baryon-baryon scattering amplitudes, the condition that all states of baryon-number two are exotic implies that the contributions to the imaginary parts of each amplitude from trajectories of opposite signatures in either crossed channel must cancel. This requires that the couplings of vector- and tensor-meson trajectories to baryons are proportional, a well-known result. The fact that the residues of Eq. (13) satisfy this proportionality condition is an attractive feature of this solution. On the other hand, if the x' of Eq. (9) were given by $-\frac{1}{3}$ or ∞ , it is seen from Eq. (6) that $x \neq x'$; so this proportionality condition would not be satisfied.

We next apply SU(3) to the s -channel residues N_i and Δ_i . The assumption that the K^+p and K^+n channels are exotic implies that all residues corresponding to the representations 10^* and 27 vanish. There are then five N -type residues: N_1, N_{10} ,

TABLE II. Predicted s -channel residues if SU(3) symmetry applies. The assumptions corresponding to the SU(3)[±] columns are (A)–(D1) of Sec. II B, SU(3) symmetry, and pattern $\Pi^+(u)$ for $K^-p \rightarrow \pi^0\Lambda$.

s -channel representation	SU(3) ⁺		SU(3) ⁻	
	N	Δ	N	Δ
10	0	-2	0	-2
ss	$-\frac{5}{4}$	$\frac{5}{4}$	$\frac{15}{4}$	$-\frac{15}{4}$
sa	$\frac{3}{4}\sqrt{5}$	$\frac{1}{4}\sqrt{5}$	$\frac{3}{4}\sqrt{5}$	$\frac{1}{4}\sqrt{5}$
aa	$\frac{15}{4}$	$-\frac{7}{4}$	$-\frac{21}{4}$	$\frac{29}{4}$
1	-4	8	12	-8

N_{ss}, N_{aa} , and N_{sa} , and five corresponding Δ -type residues. The numerical subscripts are SU(3) representations, and the lettered subscripts s and a correspond to octet residues, and denote whether the initial and final meson-baryon states are symmetric or antisymmetric in the SU(3) indices. Time-reversal invariance implies that $N_{sa} = N_{as}$ and $\Delta_{sa} = \Delta_{as}$, but since there may be more than one baryonic trajectory of the N (or Δ) type, the ss, sa , and aa residues are all taken as independent.

The pattern assignments mentioned above and the ratios of Table I may be used to determine the N and Δ in terms of the t -channel residues for the five processes π^+p, π^-p, K^-p , and K^-n scattering and $K^-p \rightarrow \pi^0\Lambda$. If Eq. (13) is used to relate the t -channel residues, one can determine all the ratios of the N and Δ . These ratios are given in Table II, for each of the two possible $K^-p \rightarrow \pi^0\Lambda$ pattern assignments.

We next consider the following four $\bar{K}N \rightarrow \pi\Sigma$ amplitudes:

$$A_1 = A(K^-p \rightarrow \pi^- \Sigma^+), \quad A_3 = A(K^-p \rightarrow \pi^0 \Sigma^0), \quad (14)$$

$$A_2 = A(K^-p \rightarrow \pi^+ \Sigma^-), \quad A_4 = \left(\frac{1}{2}\right)^{1/2} A(\bar{K}^0 p \rightarrow \pi^+ \Sigma^0).$$

All residues for these amplitudes may be determined from SU(3) symmetry, and the results compared to the pattern ratios of Table I. The results are given in the SU(3)[±] columns of Table III. It is seen that for both possible $N-\Lambda$ pattern assignments, at least one of the $N-\Sigma$ amplitudes does not correspond to a pattern.

Because of isotopic-spin invariance, only two of the above $\bar{K}N \rightarrow \pi\Sigma$ amplitudes are independent. We take these to be the amplitudes of definite isotopic spin. We also take the two independent $\pi N \rightarrow K\Sigma$ amplitudes to be those of definite isotopic spin. The predicted N_s and Δ_s for these four

TABLE III. Linear-zero patterns in A amplitudes expected from different sets of assumptions. The assumptions corresponding to the SU(3)[±] columns are those of Table II. The assumptions corresponding to the linear-zero (000) column are (A)–(D2) of Sec. II B.

Process	SU(3) ⁺	SU(3) ⁻	000
$K^-p \rightarrow \pi^- \Sigma^+$	$\Pi^-(u)$	$\Pi^-(u)$	$\Pi^-(u)$
$K^-p \rightarrow \pi^0 \Sigma^0$	no pattern		$\Pi^-(u)$
$K^-n \rightarrow \pi^- \Sigma^0$	$\Pi^+(u)$	no	$\Pi^-(u)$
		pattern	
$K^-p \rightarrow \pi^+ \Sigma^-$	$I(t)$	$I(t)$	0
$\pi^+p \rightarrow K^+ \Sigma^+$	$\Pi^-(s)$	$\Pi^-(s)$	$\Pi^-(s)$
$\pi^0p \rightarrow K^+ \Sigma^0$	no pattern		$\Pi^-(s)$
$\pi^-p \rightarrow K^0 \Sigma^0$	$\Pi^+(s)$	no	$\Pi^-(s)$
		pattern	
$\pi^-p \rightarrow K^+ \Sigma^-$	$I(t)$	$I(t)$	0

amplitudes, corresponding to the two possible $K^-p \rightarrow \pi^0\Lambda$ patterns, are shown in the SU(3)[±] columns of Table IV. The over-all normalization for the N and Δ is such that $N=1$ for π^-p scattering and $\Delta=-1$ for π^+p scattering. The experimental numbers in the table will be discussed later.

C. The linear-zero solutions

We next consider the predictions of the linear-zero hypothesis for the $N \rightarrow \Sigma$ amplitudes. Odorico has pointed out that plausible assumptions determine the zero patterns for these amplitudes¹; we sketch the argument below.

Isotopic-spin symmetry relates the amplitudes of Eq. (14) in the following manner:

$$A_3 = \frac{1}{2}(A_1 + A_2), \quad A_4 = \frac{1}{2}(A_1 - A_2). \quad (15)$$

It is assumed that the process $\pi^+p \rightarrow K^+\Sigma^+$ is dominated by Δ -type trajectories, a reasonable assumption since strongly coupled N -type resonances of these quantum numbers are not known. As can be seen from Table I, this limits A_1 to one of the three patterns: $\Pi^-(u)$, $\text{III}^-(t)$, or $\text{III}^-(s)$. The requirement that the $K^-\pi^-$ t -channel state is exotic implies that A_2 is either identically zero or corresponds to pattern I(t). Equations (8) and (15) imply that if A_2 corresponds to I(t), and A_1 to one of the three patterns mentioned above, A_3 and A_4 cannot both correspond to patterns. Hence, A_2 must be identically zero, in which case A_1 , A_3 , and A_4 correspond to the same pattern. Of the three possibilities for this pattern, $\Pi^-(u)$ is preferable, because in the other two cases every channel in every amplitude is dominated by one

signature. Such dominance is especially unrealistic in the t channel. In fact, if t -channel SU(3) is assumed, it can be shown that the t -channel residues for the processes A_1 , A_3 , and A_4 satisfy the condition $V_t = -T_t$, in agreement with pattern $\Pi^-(u)$. This is not a compelling argument, since t -channel SU(3) is inconsistent with the linear-bootstrap hypothesis for all MB processes, as shown in Sec. III. However, it is unlikely that the SU(3) symmetry of the couplings of the vector and tensor trajectories is violated so much that one of them vanishes in the $N \rightarrow \Sigma$ processes. Thus, the most plausible assignment is that suggested in Ref. 1, and listed in the column headed 000 of Table III.

The corresponding values of the N and Δ residues in amplitudes of definite isospin are listed in the 000 column of Table IV. The normalization is such as to agree with the SU(3) solutions for the amplitude $K^-p \rightarrow \pi^-\Sigma^+$ and its crossed amplitude $\pi^+p \rightarrow K^+\Sigma^+$.

V. EXPERIMENTAL RESULTS FOR $N \rightarrow \Sigma$ PROCESSES

In this section we analyze existing $N \rightarrow \Sigma$ data and compare it to the SU(3) and linear-zero predictions of Sec. IV. We discuss first the predictions concerning the zeros of the amplitudes, and later consider the values of trajectory residues.

The real and imaginary parts of the A amplitudes for the $\bar{K}N \rightarrow \pi\Sigma$ and $\pi N \rightarrow K\Sigma$ processes, computed from existing phase-shift analyses,^{6,7} are shown in Figs. 1-3. These are to be compared with the pattern predictions of Table III,

TABLE IV. Predicted and experimental ratios of residues in A amplitudes. The assumptions involved in the SU(3)[±] and linear-zero (000) columns are the same as in Table III.

Amplitude and isospin	Residue type	Experiment ^a					
		SU(3) ⁺	SU(3) ⁻	000	$j = \frac{3}{2}$	$\frac{5}{2}$	$\frac{7}{2}$
$\bar{K}N \rightarrow \pi\Sigma, I=0$	N	-1.84	1.84	-0.61		-0.88	
	Δ	1.84	-1.84	0.61	0.41		0.78
$\bar{K}N \rightarrow \pi\Sigma, I=1$	N	0.50	-2.50	-0.50		-0.28	
	Δ	-0.50	2.50	0.50	b		0.44
$\pi N \rightarrow K\Sigma, I = \frac{1}{2}$	N	1.50	-3.00	0		b	
	Δ	-1.00	3.50	0.50	b		c
$\pi N \rightarrow K\Sigma, I = \frac{3}{2}$	N	0	0	0		0.39	
	Δ	1.00	1.00	1.00	b		-0.36

^a The $\bar{K}N \rightarrow \pi\Sigma$ results are taken from Fig. 6 of Ref. 8; the $\pi N \rightarrow K\Sigma$ results are taken from the data of Ref. 7.

^b Below threshold.

^c Of the two sets of partial-wave amplitudes tabulated in Ref. 7, only the one constrained to give linear zeros has a resonating F_{17} amplitude. Because of this ambiguity, we omit this effect from the table.

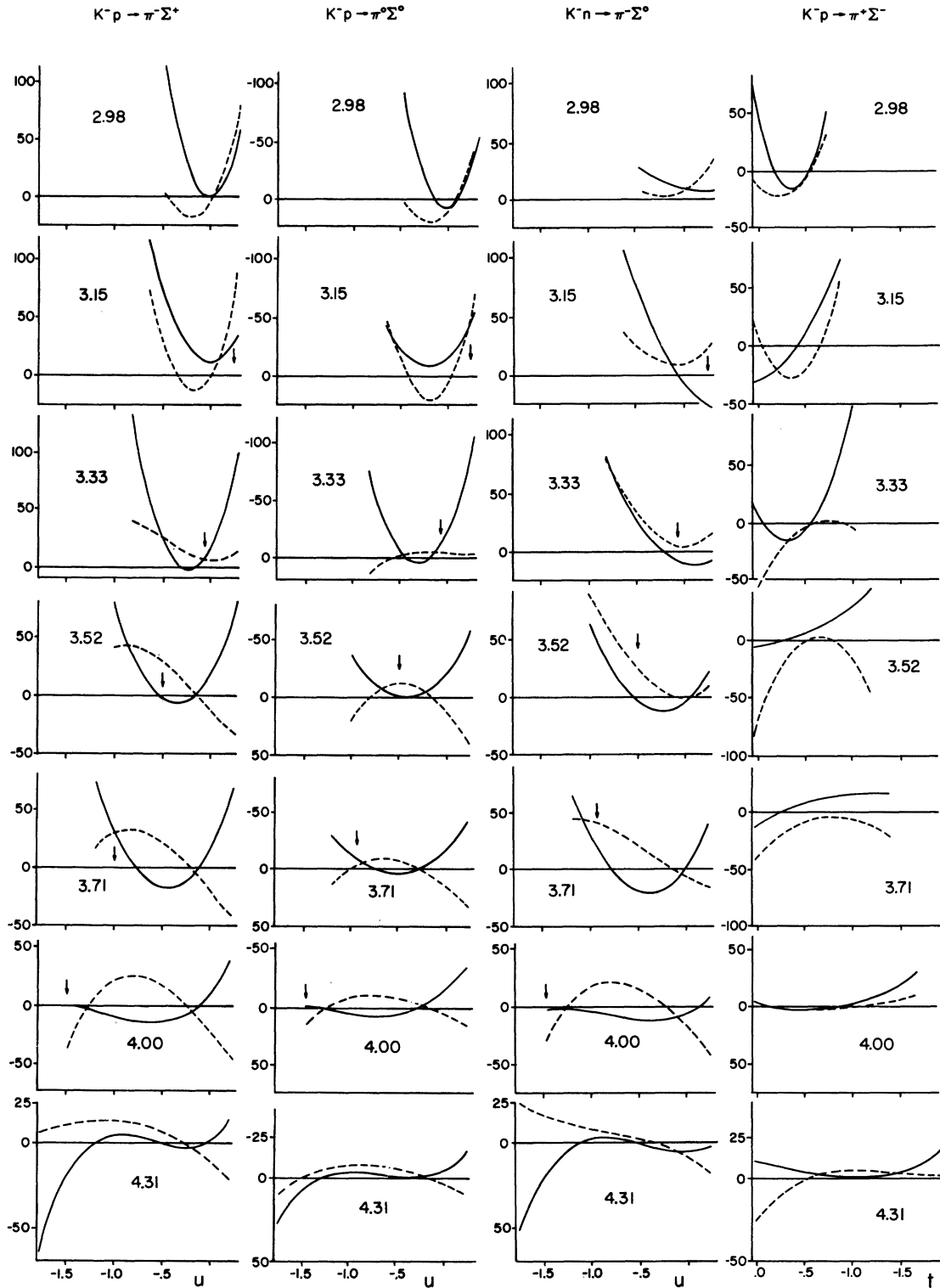


FIG. 1. Real (dashed line) and imaginary (solid line) parts of $A(s, t)$ for $\bar{K}N \rightarrow \pi\Sigma$ processes for several values of s (given inside each graph), plotted against u (against t in the $K^-p \rightarrow \pi^+\Sigma^-$ case). The units of A are GeV^{-1} and those of s, t , and u are GeV^2 . The vertical arrows correspond to $(s-t) = 4 \text{ GeV}^2$. The data are taken from solution A1 of Ref. 6 (p. 1594); the other solutions yield similar zero structures.

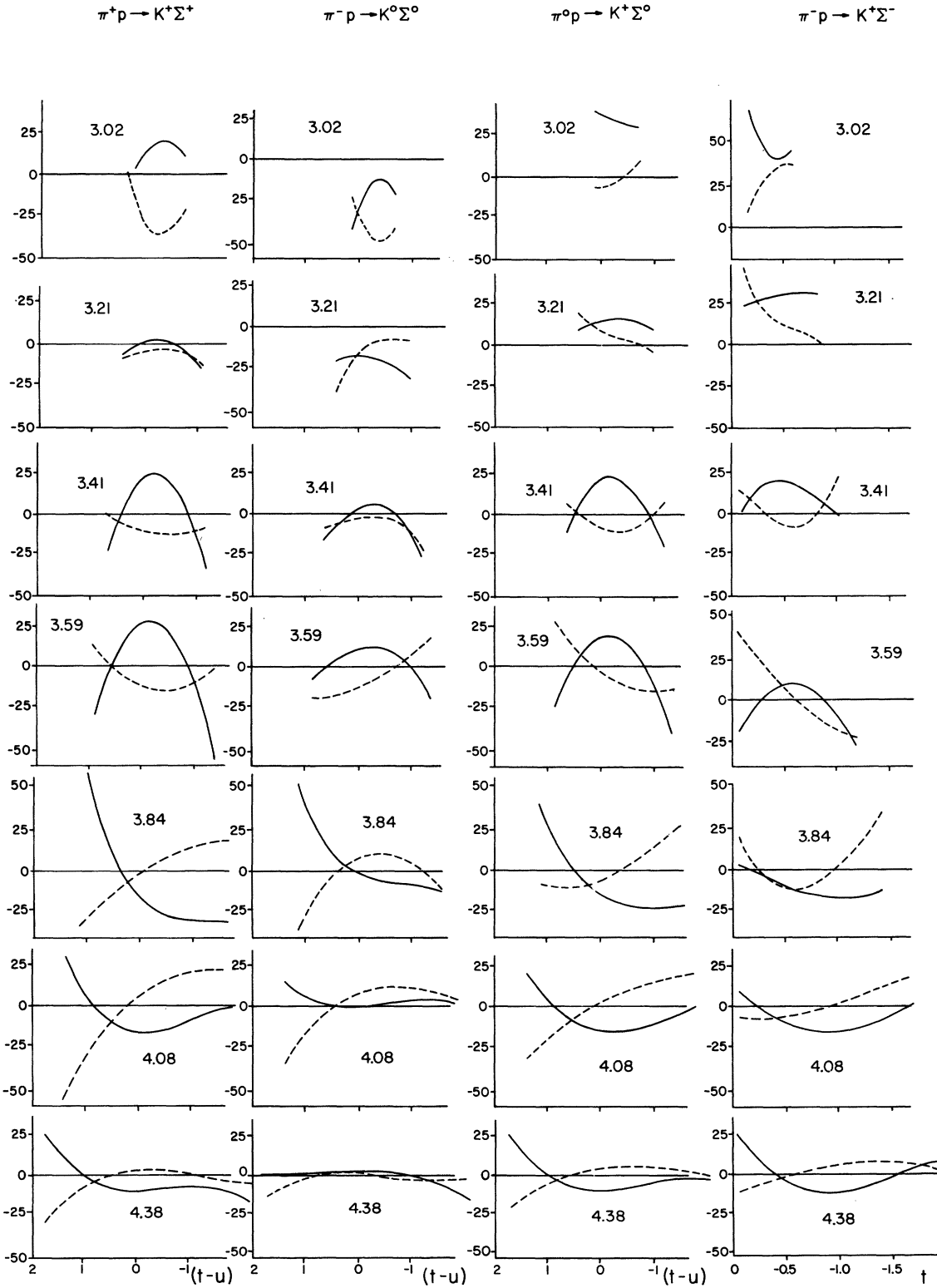


FIG. 2. Real (dashed line) and imaginary (solid line) parts of $A(s, t)$ for $\pi N \rightarrow K \Sigma$ processes for several values of s (given inside each graph), plotted against $(t-u)$ (against t in the $\pi^- p \rightarrow K^+ \Sigma^-$ case). The units of A are GeV^{-1} and those of s , t , and u are GeV^2 . The data are taken from solution II of Ref. 7.

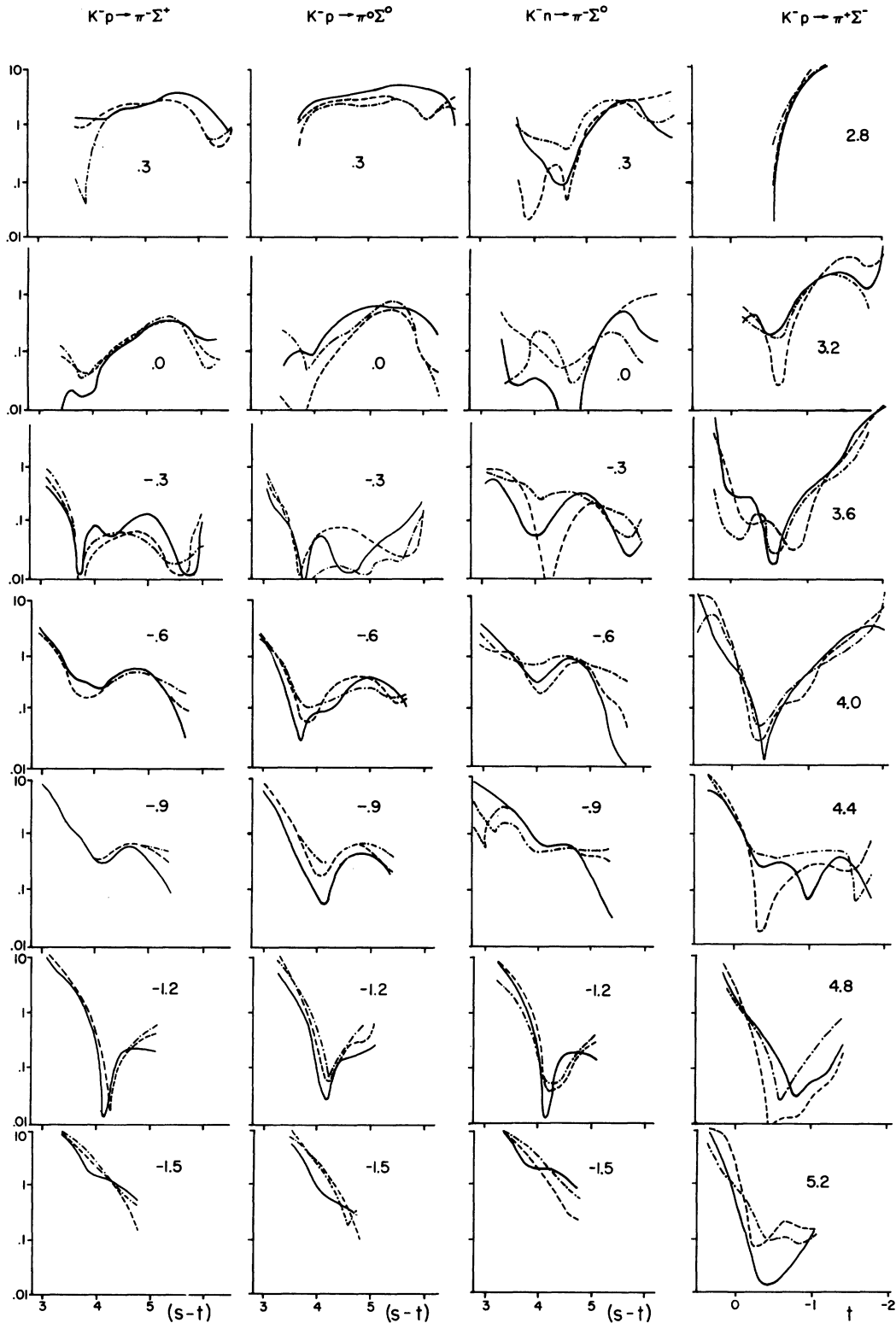


FIG. 3. $A(s,t)/N(s)$ for $\bar{K}N \rightarrow \pi\Sigma$ processes at several values of u (given inside each graph), plotted against $(s-t)$; for $K^-p \rightarrow \pi^+\Sigma^-$ the plots are against t for several values of $(s-u)$ (given inside the graphs). The units of s , t , and u are GeV^2 . $N(s)$ is the integral of $|A(s,t)|$ over the range $-1 \leq \cos \theta \leq 1$. The data are from Ref. 6; the solid, dashed, and dot-dash lines correspond to solutions A1, C1, and B2, respectively, of that paper.

and the directions of the zero lines shown in Table I.

The three sets of predictions agree on the pattern for the $K^-p-\pi^-\Sigma^+$ amplitude. The results of the phase-shift analyses for this amplitude and for the crossed amplitude $\pi^+p-K^+\Sigma^+$ are plotted for several values of s in the left-most columns of Figs. 1 and 2, respectively. In both cases, zeros of $\text{Re}A$ and $\text{Im}A$ occur close together along paths that are approximately linear in the Mandelstam plane. The lines are $u \approx -0.15 \text{ GeV}^2$ for the $K^- \rightarrow \pi^-$ reaction and $(t-u) \approx 0.5 \text{ GeV}^2$ for the $\pi^+ \rightarrow K^+$ reaction, thus supporting the predictions of Table III. The amplitude $A(K^-p-\pi^-\Sigma^+)$ is predicted to have additional zeros at constant $(s-t)$. Figure 3 shows a dip in the magnitude of this amplitude approximately along the line $(s-t) = 4 \text{ GeV}^2$. However, this dip is not associated with a simultaneous zero of the real and imaginary parts, as can be seen from Fig. 1, where the location of the dip as a function of u and s is indicated by arrows.

If one considers this dip in $|A|$, together with the zero at constant u , sufficient evidence for one of the patterns $\Pi^+(u)$, then the data on the reactions $K^-p \rightarrow \pi^0\Sigma^0$ and $K^-n \rightarrow \pi^-\Sigma^0$ support the predictions of the linear-zero hypothesis. It is shown in Fig. 1 that these amplitudes have a structure of dips and zeros similar to that of the $K^-p-\pi^-\Sigma^+$ amplitude, in agreement with the linear-zero predictions of Table III. On the other hand, the SU(3) predictions require that the three $\bar{K}N \rightarrow \pi\Sigma$ amplitudes discussed above do not have the same structure.

A similar conclusion pertains to the $\pi^-p \rightarrow K^0\Sigma^0$ and $\pi^0p \rightarrow K^+\Sigma^0$ amplitudes. Figure 2 shows that these two amplitudes have the same approximate zero at constant $(t-u)$ as does the $\pi^+p \rightarrow K^+\Sigma^+$ amplitude. This is in agreement with the linear-zero predictions of Table III, but contradicts the SU(3) predictions.

On the other hand, $A(K^-p-\pi^+\Sigma^-)$ and the crossed amplitude $A(\pi^-p \rightarrow K^+\Sigma^-)$ fit the SU(3) predictions of Table III better than the linear-zero predictions. The dip in $|A|$ for the $K^- \rightarrow \pi^+$ process occurs approximately at $t \approx -0.5 \text{ GeV}^2$ (Figs. 1 and 3). The dip in $|A|$ for the $\pi^- \rightarrow K^+$ process is not so clear-cut, but occurs approximately at $t \approx -0.3 \text{ GeV}^2$ (Fig. 2). This constant- t structure is expected for pattern I(t). Furthermore, these amplitudes are not smaller on the average than the other $\bar{K}N \rightarrow \pi\Sigma$ and $\pi N \rightarrow K\Sigma$ amplitudes, as would be expected if all leading-trajectory residues were zero for these two crossed amplitudes.

Our conclusion from the pattern analysis is that none of the three predictions of Table III fits the phase-shift analyses perfectly, but the linear-

zero prediction provides a rough fit for most of the $N \rightarrow \Sigma$ processes.

We now turn to the experimental residue ratios, compared to the predicted ratios in Table IV. The experimental predictions of the right-hand columns are the contributions of N - and Δ -type resonances to the residues of the A amplitude for the $N \rightarrow \Sigma$ processes. The contribution of each resonance is proportional to the imaginary part of the relevant partial-wave amplitude at the resonance energy, multiplied by the resonance width. If all contributions to the same residue were proportional, as assumed in Sec. II A, these residues could be compared at any momentum transfer. This proportionality assumption is not exactly valid, however, because two different partial waves contribute to some residues. (For example, $D_{5/2}$ and $F_{5/2}$ resonances contribute to the same residue.) Ideally, one should compute these residues at positive t values near those of the t -channel resonances, since Odorico's residue-ratio conditions are obtained at resonance intersections. Fortunately, if t is appreciably positive, the partial wave of higher l dominates, so the exact value of t that is chosen is not important. We have chosen $t = 1 \text{ GeV}^2$ for the $\pi N \rightarrow K\Sigma$ resonances, and have taken the $\bar{K}N \rightarrow \pi\Sigma$ residue ratios from a recent analysis of Odorico.⁸ The normalization for each j is such that the $(j = \frac{5}{2})$ N -type residue for π^-p scattering is 1, and the $(j = \frac{3}{2}$ and $\frac{7}{2})$ Δ -type residues for π^+p scattering are -1 . The πN phase-shift analysis used in the normalization is that of Almeded and Lovelace.⁹

The magnitudes of the residue ratios are expected to be sensitive to the SU(3) mass splitting of the external particles, especially in the cases of higher angular momenta. Therefore, we will stress the comparison of the predicted and experimental signs of these ratios. It is seen from Table IV that whether or not the over-all sign is changed, the measured $\bar{K}N \rightarrow \pi\Sigma$ residues are in clear contradiction to both sets of SU(3) predictions. On the other hand, these measurements agree in sign and approximately in magnitude with the linear-zero predictions. The table also shows that all the predictions fail to reproduce the residues for the $\pi N \rightarrow K\Sigma$ processes very accurately.

We conclude that although the evidence is not clear-cut, the present data favor the linear-zero postulate to SU(3) symmetry for the $N \rightarrow \Sigma$ spin-independent amplitudes. In order to make the meaning of this conclusion clear, we summarize the procedure briefly. Odorico has shown that the linear-zero postulate for the spin-independent amplitudes is supported by data on πN and $\bar{K}N$ scattering and the process $\bar{K}N \rightarrow \pi\Lambda$.^{1,2} Consequently, we have applied the postulate to these

amplitudes. If SU(3) interaction symmetry is assumed also, there are only two solutions for the interaction ratios; in each of these all the ratios are determined. Data on the $N \rightarrow \Sigma$ processes are in strong contradiction to both these solutions.

Clearly, if the linear-zero postulate were not applied to any amplitude, the SU(3) violation would be less clear-cut. This is because the data analyzed by Odorico contain experimental uncertainties, so that if no supplementary postulate were

used, the $N \rightarrow \Sigma$ predictions would not be so precise. The significant thing about our results is not the SU(3) violation, but the experimental suggestion that nature prefers the less-well-known linear-zero postulate to SU(3) symmetry for spin-independent amplitudes. More data and phase-shift analyses of the $\bar{K}N \rightarrow \pi\Sigma$ and $\pi N \rightarrow K\Sigma$ amplitudes are needed to test this suggestion more thoroughly.

*Work supported in part by the U. S. Atomic Energy Commission.

¹R. Odorico, Phys. Lett. **41B**, 339 (1972).

²R. Odorico, Nucl. Phys. **B37**, 509 (1972).

³R. Odorico, Phys. Lett. **38B**, 37 (1972).

⁴R. H. Capps, Phys. Rev. **D 7**, 3394 (1973).

⁵In Ref. 1, it is stated that the linear-zero assumption (together with the other assumptions of Sec. II B of the present paper) is consistent with t -channel SU(3) if SU(3) is not applied in the s or u channels. This is incorrect, as shown by the argument given here.

⁶Daniel F. Kane, Jr., Phys. Rev. **D 5**, 1583 (1972).

⁷W. Langbein and F. Wagner, Nucl. Phys. **B53**, 251 (1973).

⁸R. Odorico, in *Baryon Resonances—73* (Purdue Univ. Press, West Lafayette, Indiana, 1973), pp. 135–147. In this reference, the $\bar{K}N \rightarrow \pi\Sigma$ residue ratios are averages over several phase-shift analyses, and are shown in Fig. 6. This is a more up-to-date version of Fig. 2 of Ref. 1.

⁹S. Almeded and C. Lovelace, Nucl. Phys. **B40**, 157 (1972).

Physical trajectories in an inclusive dual resonance model*

J. Randa†

Physics Department, University of Illinois at Urbana-Champaign, Urbana, Illinois 61801

(Received 3 December 1973)

Previous work on the dual resonance model in inclusive vector-meson production is extended to include both abnormally coupled trajectories and trajectories with positive intercept. Differential cross sections and density-matrix elements are obtained and compared to those of the previous calculation. The single-particle spectrum for spinless mesons is also obtained and compared with earlier results.

I. INTRODUCTION AND NOTATION

A. Introduction

In a previous paper¹ the predictions of a standard dual resonance model (DRM) for inclusive vector-meson production were obtained. The calculation had two major shortcomings which one could expect to overcome within the framework of a DRM. The first is that the B_s which was used² contains only normal [for $1+2 \rightarrow 3$, $\eta_s = \eta_1\eta_2$, where $\eta_i = (-1)^{J_i}P_i$] couplings. Consequently, for $\pi N \rightarrow \rho X$, where X is anything, only π exchange is included in the t ($\pi\bar{p}$) channel. But at very high energies one would expect A_2 exchange to become increasingly important (due to its higher intercept), and we would therefore like to include abnormally

coupled trajectories in the calculation. The second unpleasant feature was the use of only one internal trajectory, the “ π - ρ ” trajectory $\alpha(s) = -m_\pi^2 + s$. While this is not expected to be a fatal flaw, it is desirable to investigate the predictions of a more “physical” model, for the sake of comparison to both experiment and to the predictions of the simpler model.

In this paper we remedy these two ills. Using the kinematic superstructures of Canning and Jacobs,³ we construct an amplitude with abnormal coupling to accommodate the A_2 trajectory. Provision for trajectories with positive intercepts is made by using the tachyon-free amplitude of Rittenberg and Rubenstein.⁴ The one-particle spectra and density matrices of π and A_2 exchange